Flow Performance of High-Fluidity Concrete

Zhuguo Li[1]; Taka-aki Ohkubo[2]; and Yasuo Tanigawa[3]

Abstract: In this paper a particle assembly model was proposed for high fluidity concrete in the fresh state. This particle assembly is composed of cohesionless particles (aggregates grains) and cohesive particles (cement grains) surrounded by mixing water membranes. By using a microscopic approach and expanding Eyring's rate process viscosity theory, the flow mechanism of high fluidity concrete having interfriction was clarified, and its flow curve was examined. Furthermore, the effects of normal stress and environmental temperature on the flow behavior of high fluidity concrete were investigated quantitatively. Finally, a shear test apparatus was developed and a series of shear tests were performed to verify the obtained theoretical results.

DOI: 10.1061/(ASCE)0899-1561(2004)16:6(588)

CE Database subject headings: Concrete; Fluid flow; Particle interactions; Viscosity.

Introduction

Due to having a self-compacting characteristic, high fluidity concrete can be expected to play an important role in minimizing labor and improving concrete durability. Sufficient workability is required for high fluidity concrete to ensure that structural elements or members, with given geometries and reinforcing bar contents, can be successfully cast without vibration. The process of selecting the workability of fresh concrete is called workability design of concrete, of which the prop is numerical flow simulation, as shown in Fig. 1 (Tanigawa and Mori 1988). To perform the flow simulation, the flow behavior of high fluidity concrete must first be clarified (Mori 1998).

Several different types of rheological test devices have been developed for fresh concrete by other researchers (e.g., Banfill 1990; Wallevik and Gjørv 1990; Struble and Schultz 1993; Hu and Larrad 1996; and Yamamoto et al. 1996), but there is not a generally accepted method for testing the flow performance of fresh concrete. The cement hydration and the material segregation during testing produce undesirable effects on the test results. Hence, it is difficult to accurately examine the flow behavior of fresh concrete by the experiments, and the flow performance of high fluidity concrete is not yet fully clarified and quantified at present.

In the present rheological studies of fresh concrete, fresh concrete is regarded as a homogeneous continuum, and its shear flow behavior is usually characterized by the Bingham model, which describes the variation of shear rate with shear stress by a linear relationship (Tattersall and Banfill 1983). However, while high fluidity concrete flows through reinforcing bars, it is unreasonable to assume that all particles in fresh concrete are not continuously in contact. The interparticle contacts will cause interparticle friction that increases the flow resistance of fresh concrete. Thus the flow resistance increases with the normal stress on the shear plane (Mori et al. 1991). Moreover, the flow performance of high fluidity concrete changes with elapsed time of flow or agitation, which is called thixotropy phenomenon (Papo 1988; Banfill 1991; Struble and Schultz 1993). However, the Bingham model is invalid in describing the normal stress dependence and the thixotropy of the flow behavior for high fluidity concrete.

In this study, a microscopic approach is taken to the flow performance of high fluidity concrete. A particle assembly model is proposed for fresh concrete, and its flow mechanism is clarified for the condition where its granular material character is also taken into account together with its liquid character. Then, the flow curve equation of high fluidity concrete and the effects of concrete's composition, normal stress, and environmental temperature on its flow behavior are investigated.

Particle Assembly Model

Fresh concrete, which is often thought to have a visco-plastic body, is actually a type of particle assembly composed of water, cement grains, and aggregates grains. Almost all particles make contact with adjacent particles. The particles that are completely separate in the initial state will push aside the surrounding water, and also come in contact with others when they move. As shown in Fig. 2, the contact slant of particles is not generally parallel to the maximum shear (MS) plane and changes with the particle positions. The angle between the contact slant and the direction of the MS plane is expressed as θ_i, referred to as particle contact angle. The fabric of the particle assembly can be described by the distribution and the mean value (θ_m) of θ_i (Murayama 1991).

In this investigation, it is assumed that each particle contacts the others at only one point on a given MS plane. If there is more than one contact point, an imaginary one is used to integrate all of them. As a result, the number of the contact points becomes equal to that of the particles on the same MS plane. The number of

[1]Researcher, Graduate School of System and Information Engineering, University of Tsukuba, 1-1-1, Tenoudai, Tsukuba, Ibaraki, 305-0802, Japan.

[2]Professor, Dept. of Social and Environmental Engineering, Graduate School of Engineering, Hiroshima University, 1-4-1, Kagamiyama Higasi-Hiroshima, 739-8527, Japan

[3]Professor, Department of Architecture, Graduate School of Science and Technology, MeijoUniversity, 1-5-1 Shiogamaguchi, Tempaku-ku, Nagoya, 468-8502, Japan

Note. Associate Editor: Kimberly E. Kurtis. Discussion open until May 1, 2005. Separate discussions must be submitted for individual papers. To extend the closing date by one month, a written request must be filed with the ASCE Managing Editor. The manuscript for this paper was submitted for review and possible publication on October 31, 2002; approved on January 5, 2004. This paper is part of the ***Journal of Materials in Civil Engineering***, Vol. 16, No. 6, December 1, 2004. ©ASCE, ISSN 0899-1561/2004/6-588–596/$18.00.

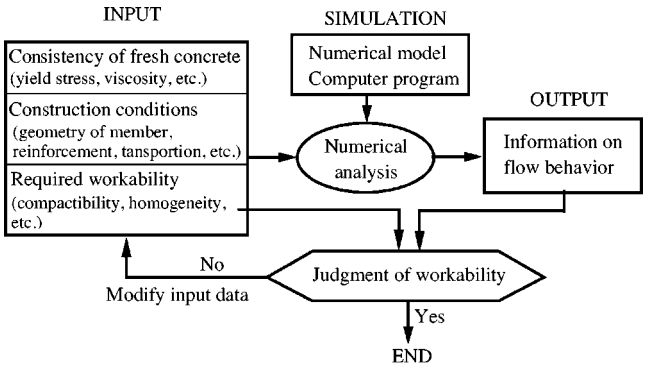

Fig. 1. Workability design approach of concrete based on numerical flow simulation

contact points on a unit dimension of the MS plane is expressed as N.

The contact between particles results in the interparticle friction that is thought to follow Coulomb's solid friction law. Hence, whether the particles in fresh concrete are stationary or moving, all the cement particles and the aggregate particles are subjected to interfrictional resistance.

Besides van der Waals attraction force, there also is a static electric repulsive force between the cement particles when adding naphthalene sulfonate-based superplasticizer, or a steric hindrance when mixing a polycarboxylate-based one (Fukaya 1992, Sakai and Dimon 1996; Uchikawa et al. 1997). Any interaction or total potential energy of cement particle changes with interparticle distance, as shown in Fig. 3 (Everett 2000). This interparticle potential energy becomes an energy barrier to obstruct the cement particle from moving, and results the movement of the cement particle becoming time dependent as discussed in detail in the next section.

A stationary cement particle is approximately in equilibrium with attractive forces and repulsive forces from its surrounding particles, so it is subjected only to the interfrictional resistance. However, when the cement particle moves, it also meets other type of resistance, caused by the breakdown of the attraction–repulsion equilibrium (hereafter referred to as viscous resistance). To create a moving particle, the interparticle force must first destroy the links of atoms or molecules on the particle interfaces that contribute to the interparticle solid friction (Murayama 1991). Only when the particle is moving relative to its neighboring particles does a viscous resistance result from the interparticle potential energy (also called potential energy barrier) to obstruct the particle movement.

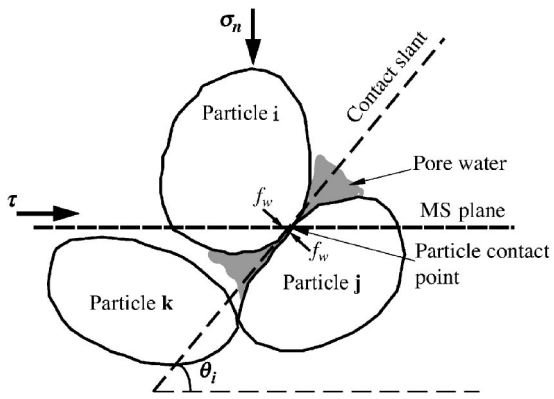

Fig. 2. Particle contact slant and particle contact angle

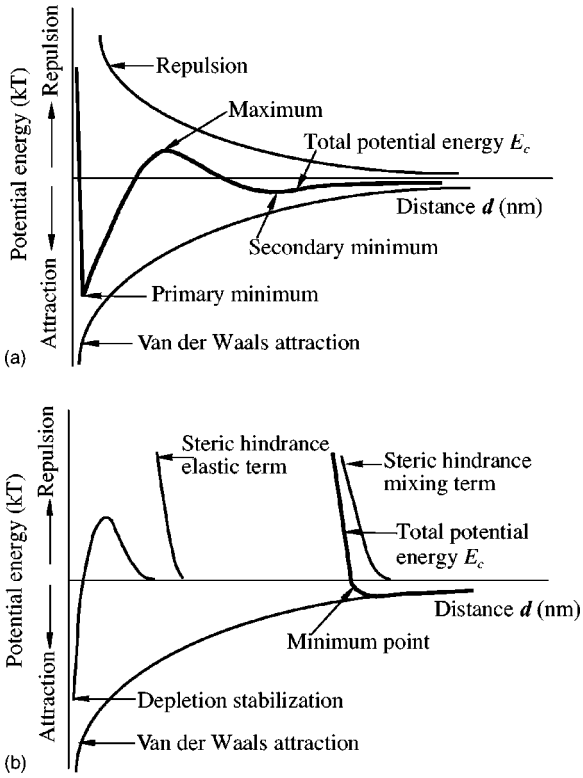

Fig. 3. Potential energy of intercement particle when adding superplasticizer: (a) naphthalene sulfonate based and (b) polycarboxylate based

Hence, a moving cement particle has to meet with the frictional and viscous resistances, and a static cement particle starts to move only when its subjected static frictional and viscous resistances are both overcome by its interparticle force. However, because there is no diffusive electric double layer around aggregate particles, and aggregate particles can not absorb superplasticizier on their surfaces, moving aggregate particles are only subjected to the interfrictional resistance.

Therefore, as a kind of particle assembly, fresh concrete contains two particle groups—a cohesive particle group (cement grains) and a cohesionless particle group (sand and gravel grains). In the static state, both the particle groups are only subjected to the frictional resistance, but in the moving state, only the former simultaneously bears the viscous resistance together with the frictional resistance.

The maximum shear stress τ_{max}, supported by the interfrictional resistance of particle assembly without deformation, is given by the following equation (Shimada et al. 1993; Li 2001; Li et al. 2001):

$$\tau_{max} = \sigma_n \tan(\theta_m + \phi_m) + \frac{N f_{wm} \tan \phi_m}{\cos \theta_m (1 - \tan \theta_m \tan \phi_m)} \quad (1)$$

where σ_n=normal stress on MS plane; θ_m=mean particle contact angle; ϕ_m=mean interfrictional angle; and f_{wm}=mean adhesive force acting on the particle contact point, which is caused by the surface tension and suction of mixing water as shown in Fig. 2.

Since the distribution of interparticle forces is affected by many factors such as particle's position, shape, and size, their

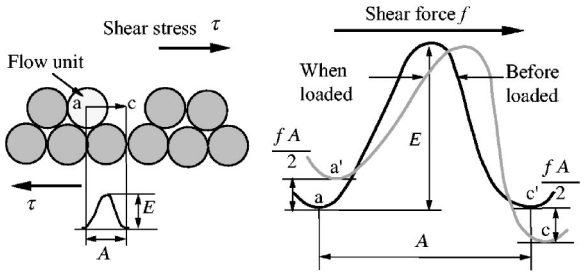

Fig. 4. Relationship between particle movement and shear deformation of particle assembly

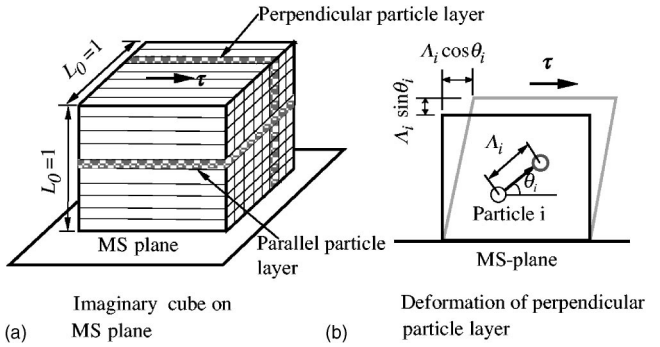

Fig. 5. Microscopic view of viscous flow of matter under external force

measurement or numerical estimation is impossible at present. But it is reasonable to consider that a larger particle bears a greater interparticle force because it generally has a larger cross section. Hence, if we ignore the ability of pore water and air in the particle assembly to support external force by their viscous resistances and suppose that the stress portion (τ_c) imposed on the cement particle group is proportional to the volume ratio of the cement particles to all the solid particles, τ_c is expressed by the following equation when a shear stress (τ) is applied to the particle assembly:

$$\tau_c = \frac{V_c}{V_c + V_a} \cdot \tau = S_d \tau \tag{2}$$

where V_c and V_a=volumes of cement particles and aggregate particles in a unit volume of concrete (m^3/m^3), respectively; and S_d=stress distribution coefficient ($=V_c/(V_c+V_a)$).

Flow Mechanism

As shown in Fig. 4(a), the particle assembly is imagined to comprise a cube with sides of unit dimension on the MS plane, and the MS plane is acted on by a shear stress τ. This imaginary cube is composed of many particle layers that are perpendicular or parallel to the MS plane. The thickness of any particle layer is equal to the maximum particle diameter in this particle layer. From the probabilistic viewpoint, the mechanical behaviors of the particles in any perpendicular particle layer is the same as that in the others, and the shear deformation of any vertical particle layer is equal to that of this cube.

Under a shear stress τ, the movement of any a particle i will result in an obliqueness $\Lambda_i \cos\theta_i$ in its locating vertical particle layer [Fig. 4(a)]. When n particles move in the vertical particle layer, the shear deformation of the imaginary cube, i.e., the shear strain (γ) on the MS plane, is expressed by the following equation (Murayama 1991; Li et al. 1999):

$$\gamma = \sum_{i=1}^{n} \frac{1}{L_0} \cdot \Lambda_i \cdot \cos\theta_i = n \cdot \Lambda_m \cdot \cos\theta_m \tag{3}$$

where Λ_i=moving distance of particle i; and Λ_m=mean moving distance of n particles.

Eyring's well-known viscosity theory (Goto 1963) has already been applied successfully to explain the viscosity of non-Newtonian fluids, colloids, and soils (Murayama 1991). According to this theory, when loaded by an external force, some tiny constitutional particles of atomic or molecular scale, which are referred to as flow units, gain enough kinetic energy to surmount each potential energy barrier and move to vacant spaces in the matter (Fig. 5). The deformation or flow of matter results from the movements of flow units, and the deformation or flow rate depends on the number of flow units in a unit time and their mean moving distance (Λ). The occurrence probability (P) of the flow units in unit time is given by

$$P = 2A \sinh\left(\frac{f \cdot \Lambda}{2kT}\right)$$
$$A = \frac{kT}{h}\exp\left(-\frac{E}{kT}\right) \tag{4}$$

where f=mean shear force acting on a flow unit (N); E=height of potential energy barrier (J); T=absolute temperature (K); k=Boltzmann's constant (1.380662×10^{-23} J/K); and h=Planck's constant ($6.6260755 \times 10^{-34}$ J/s).

If an individual moving cement particle is considered to be a flow unit, Eyring's viscosity theory can be applied to describe the flow behavior of the cement particle group. However, as stated above, only when the subjected interfrictional resistance can be overcome does a cement particle have a chance to match further the subjected viscous resistance and to become a moving particle. Here, a cement particle, whose interparticle force is larger than its subjected frictional resistance, is called a potential active (PA) particle. From the probabilistic viewpoint, the number (N_{ca}) of PA particles is the same in each particle layer, whether perpendicular or parallel. Hence, the moving cement particle is a special PA particle, whose kinetic energy is the sum of the Brownian motion energy and the energy gained from external force and is large enough to surmount its interparticle energy barrier resulting from its subjected viscous resistance and interfrictional resistance.

By applying Eyring's viscosity theory, the mean probability (P_c) that PA particles become moving cement particles in unit time is expressed by the first equation in the following equation. Thus, the number (n) of moving cement particles in a particle layer in unit time is obtained by the third equation as follows:

$$P_c = 2A \sinh\left(\frac{f_v \cdot \Lambda_{cm}}{2kT}\right)$$
$$A = \frac{kT}{h}\exp\left(-\frac{E_c}{kT}\right) \tag{5}$$
$$n = N_{ca} \cdot P_c$$

where Λ_{cm}=mean moving distance of cement particles; E_c=mean potential energy of cement particles (J); and f_v=mean shear force

used to match the viscous resistance imposed on a PA particle, and is given by

$$f_v = (\tau_c - \tau_{cf})/N_{ca} \tag{6}$$

where τ_{cf}=shear stress used to match the frictional resistance of the cement particle group.

Eq. (5) indicates that the number of moving cement particles in a particle layer varies with elapsed time. Thus the moving behavior of the cement particle group should have a time-dependent characteristic. However, since the movement of the aggregate particle is not exposed to the potential energy barrier, the occurrences of moving aggregate particles are time independent. Therefore, the deformation of the aggregate particle group is an instantaneous deformation that does not result in a shear rate in the particle assembly. If assuming that the cement particle group and the aggregate particle group separately contribute shear strains to the particle assembly by their movements, the shear strain rate ($\dot{\gamma}$) of fresh concrete depends on the movement of the cement particles, and is expressed by the following equation according to Eqs. (3) and (5):

$$\dot{\gamma} = N_{ca} \cdot P_c \cdot \Lambda_{cm} \cdot \cos\theta_{cm} \tag{7}$$

where θ_{cm}=mean contact point angle of moving cement particles.

Therefore, the apparent viscosity η_a of fresh concrete is

$$\eta_a = \frac{\tau}{2AN_{ca}\Lambda_{cm}\cos\theta_{cm}\sinh\left[\dfrac{(\tau_c - \tau_{cf})\cdot\Lambda_{cm}}{2kTN_{ca}}\right]} \tag{8}$$

Eq. (8) shows that the apparent viscosity of fresh concrete depends on shear stress, environment temperature, its composition, and particle fabric. This apparent viscosity not only expresses the liquid character of fresh concrete, but also integrates the effects of its granular character through the parameters of θ_{cm}, Λ_{cm}, and τ_{cf}, etc.

Shear Flow Characteristic

Flow Curve

As a particle assembly, fresh concrete supports external force by interfrictional resistance, viscous resistance, and the resistance that is caused by the dilatancy of fresh concrete (hereafter called dilatancy-caused resistance) (Li et al. 2001, Murayama 1991). The interfrictional resistance depends on the normal pressure on particle contact plane and the interparticle frictional angle according to Coulomb's friction law. The dilatancy-caused resistance depends on the particle contact angle (Murayama 1991). The feature of high fluidity concrete, which can flow by its gravity, means that its total inter-resistance is very small. That is, ϕ_i and θ_i are small, and most of the cement particles become the PA particles when a shear stress of more than τ_y is applied. Hence, the following approximations can be made:

$$\theta_m \approx 0$$

$$\theta_{cm} \approx 0 \tag{9}$$

$$N_{ca} \approx N_c$$

where N_c=number of cement particles in a vertical particle layer with unit dimension.

According to the rheological definition of yield stress, the yield stress of fresh concrete is a limit shear stress, above which the shear strain rate can be measured. Since the movements of only the cement particles will result in a shear strain rate in fresh concrete as stated above, there are cement particles that move in fresh concrete only when the applied shear stress is greater than the yield stress. Moreover, because only moving cement particles are subjected to viscous resistance, the yield stress is also regarded as a limit stress, within which there is not viscous resistance in fresh concrete. Hence, the yield stress is equivalent to the sum of static interfrictional resistance and dilatancy-caused resistance. When approximating the mean particle contact angle to zero and ignoring the difference between the static frictional angle and the dynamic one, the dilatancy-caused resistance becomes zero and the interfrictional resistance is a constant for a given specimen. Thus, the yield stress (τ_y) of high fluidity concrete in a fresh state is expressed approximately by the following equation derived from Eq. (1):

$$\tau_f \approx \sigma_n \tan\phi_m + Nf_{wm}\tan\phi_m \tag{10}$$

Because the stationary cement particles in high fluidity concrete support the applied external force by their interparticle friction, the maximum interfrictional resistance τ_{cf} of the cement particle group should be expressed as

$$\tau_{cf} = S_d \cdot \tau_y \tag{11}$$

According to Eyring's viscosity theory, the number of flow units increases with increasing shear stress, and the moving distance of flow unit before it reaches a new equilibrium position is dependent on only the distribution of vacant space. The moving distances of individual cement particles in fresh concrete should be different from others, but their mean value (Λ_{cm}) is assumed to be a constant for simplifying this investigation.

Substituting Eqs. (2), (6), (9), and (11) into Eq. (7), the shear strain rate of high fluidity concrete is obtained as

$$\dot{\gamma} = c_1 \exp\left(-\frac{E_c}{kT}\right)\sinh[c_2(\tau - \tau_y)] \tag{12}$$

where

$$c_1 = \frac{2kT}{h}N_c\Lambda_{cm}$$

and

$$c_2 = \frac{S_d\Lambda_{cm}}{2kTN_c}$$

Eq. (12) shows that the flow rate of high fluidity concrete increases with shear stress, the flow curve is drawn as shown in Fig. 6, with a shape that agrees with general knowledge about the flow curve of suspension (Onogi 2000).

Thus, the apparent viscosity (η_{ah}) of high fluidity concrete is expressed by

$$\eta_{ah} = \frac{\tau}{c_1}\exp\left(\frac{E_c}{kT}\right)\frac{1}{\sinh[c_2(\tau - \tau_y)]} \tag{13}$$

When $c_2(\tau - \tau_y)$ is not more than 1, i.e., the shear flow is in a low rate range, Eq. (12) can be simplified to the second equation below based on the approximation shown in the first equation. In this case, the Bingham model may characterize the shear flow behavior of high-fluidity concrete

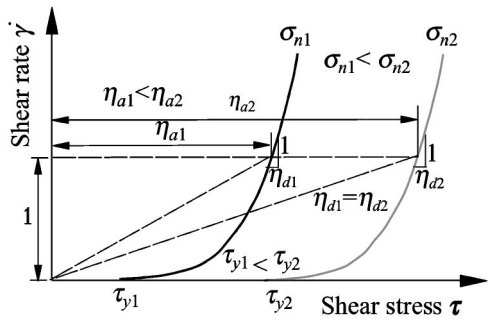

Fig. 6. Flow curve of high fluidity concrete and effect of normal stress

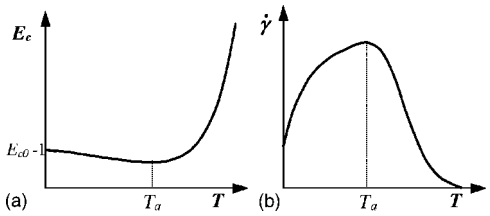

Fig. 7. Relationship between mean potential energy of cement particles (a) or shear rate (b) of high fluidity concrete and temperature

$$\sinh[c_2(\tau - \tau_y)] \cong c_2(\tau - \tau_y) \tag{14}$$

when

$$c_2(\tau - \tau_y) \leqslant 1$$

$$\tau = \dot{\gamma} \cdot \left[\frac{h}{S_d \Lambda_{\text{cm}}^2} \exp\left(\frac{E_c}{kT} \right) \right] + \tau_y \tag{15}$$

But when $c_2(\tau - \tau_y)$ is not less than 2, Eq. (12) can be approximated from the second equation as follows because an approximation shown in the first equation can be made. That is to say, when the shear flow is in the high rate range, the flow curve is the exponential graph

$$2 \sinh[c_2(\tau - \tau_y)] \cong \exp[c_2(\tau - \tau_y)] \tag{16}$$

when

$$c_2(\tau - \tau_y) \geqslant 2$$

$$\dot{\gamma} = \frac{1}{2} c_1 \exp\left(- \frac{E_c}{kT} \right) \exp[c_2(\tau - \tau_y)] \tag{17}$$

Effect of Normal Stress

By substituting Eq. (10) into Eq. (12), the following equation is obtained as

$$\dot{\gamma} = c_1 \exp\left(- \frac{E_c}{kT} \right) \sinh\{c_2[\tau - \sigma_n \tan \phi_m - N f_{\text{wm}} \tan \phi_m]\} \tag{18}$$

Eq. (18) shows that with increasing normal stress σ_n on the shear plane, the shear rate of high fluidity concrete decreases. According to Eq. (10), with increasing σ_n, the yield stress will increase linearly. In this case, the shear stress used to match the viscous resistance of cement particles decreases, and the flow rate drops accordingly.

Hence, as shown in Fig. 6, with an increase in normal stress ($\sigma_{n2} > \sigma_{n1}$), the flow curve shifts toward increasing shear stress ($\tau_{y2} > \tau_{y1}$), and the apparent viscosity increases ($\eta_{a2} > \eta_{a1}$), but the curvature of the flow curve [i.e., differential viscosity ($\eta_d = d\tau/d\gamma$)] doesn't change ($\eta_{d2} = \eta_{d1}$).

Effect of Temperature

Right after concrete is mixed, the mean potential energy of cement particles (E_c) is expressed by the following equation when the effect of the hydrates is considered (Li et al. 2002). The second term on the right of the equation represents an increase in the potential energy, mainly caused by the hydration of C_3A during which concrete is mixed

$$E_c = E_{c0} + \left(1 - \left\{ 1 - t_0 \cdot S_{20} \cdot \exp\left[B \cdot \left(\frac{1}{293} - \frac{1}{T} \right) \right] \right\}^3 \right) \tag{19}$$

where E_{c0} = mean potential energy of cement particles in the initial period when there are no the hydrates; t_0 = mixing time of concrete; S_{20} = constant for describing the hydration rate of C_3A at 20°C; and B = constant. E_{c0} = difference between van der Waals attraction energy and repulsive energy, and is expressed by the following equation when adding polycarboxylate-based superplasticizer (Japan Rheology Society 1992):

$$E_{c0} = \frac{1}{N_c} \cdot \sum_{i=1}^{N_c} (V_{\text{vi}} - V_{\text{si}}) \tag{20}$$

where V_v = van der Waals attraction energy; and V_s = steric hindrance energy.

V_v and V_s are given in the following two equations, respectively (Japan Rheology Society 1992; Sakai and Dimon 1996; Nakae 2001):

$$V_v = - \frac{A}{12\pi D^2} \tag{21}$$

where A = Hamaker's constant; and D = interparticle distance, and

$$V_s = \omega_1 m^2 kT \left(1 - \frac{390}{T} \right) + \omega_2 kT \tag{22}$$

where m = the amount of the polymers absorbed on unit cement particle surface; and ω_1 and ω_2 = two parameters that are related to the structural character and the absorption amount of polycarboxylate-based superplasticizer, cement particle radius, and the minimum intercement particle distance, etc., but whose numerical expressions are not given here because they are very complicated.

The amount of the absorbed superplasticizer is affected by environmental temperature (T), but the quantitative relationship between them is not yet clear. When this effect of the variation of the absorption amount of superplasticizer with T on the steric hindrance energy is ignored, the steric hindrance potential energy (V_s) increases with rising T according to Eq. (22). Thus the mean potential energy (E_{c0}) of cement particles in the initial period decreases with T.

On the other hand, since the hydrate generation increases with raising T, the density and thickness of the polymer absorption layer decrease, and the V_s thus declines. That is to say, when increasing T, the first term (E_{c0}) on the right of Eq. (19) decreases, but the second term increases. Hence, as shown in Fig.

Table 1. Mixture Proportions of High Fluidity Cementitious Materials

Mixture	Cement paste	Mortar	Concrete
W/C	0.45	0.45	0.45
S/C	0	1.64	1.64
$S/(S+G)$	0	0	0.45
Water, W (kg/m^3)	582.9	318.4	212.0
Portland cement, C (kg/m^3)	1,295.3	706.6	471.0
Silica sand, S (kg/m^3)	0	1,161	772.6
Glass ball, G (kg/m^3)	0	0	944.4
Superplasticizer, ($C\times$ %)	0	1.5	1.8

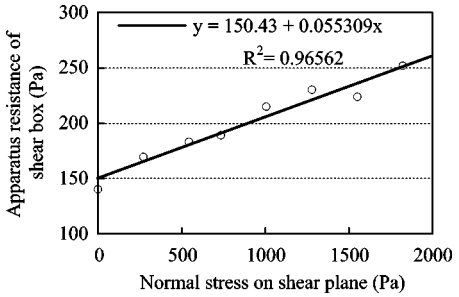

Fig. 9. Apparatus resistance of shear box under different normal stress

7(a), the interparticle potential energy (E_c) linearly decreases with T, but once the T rises above a certain limit (T_a), the E_c turns inversely to increase with the T in an exponential relationship.

The smaller the interparticle potential energy, the easier it is to create a moving cement particle, and thus the greater the $\dot{\gamma}$ becomes. The variation of the shear rate of high fluidity concrete with T can be clarified based on Eq. (12). The variations of E_c, c_1, and c_2 in Eq. (12) with T are not the same, c_2 decreases with increasing T as opposed to E_c and c_1. But since the increasing rate of $c_1 \exp(-E_c/kT)$ is larger than the decreasing rate of $\sinh[c_2(\tau-\tau_y)]$, the finality is that how the $\dot{\gamma}$ of high fluidity of concrete varies with T depends on the variation of E_c and is shown as Fig. 7(b) for a certain shear stress.

Experimental Investigation

Constituent Materials

Mixture proportions of the high fluidity cement paste, mortar, and concrete used are shown in Table 1. In order to avoid bad effects of aggregate quality fluctuation on test results, Japanese Industry Standard (JIS) No. 6 silica sand (size: 0.1–0.5 mm) was used as fine aggregate, and glass balls were used as coarse aggregate. The glass balls were of four diameters: 5, 7, and 10 mm, with a volume ratio 1.0: 0.6: 0.3. To avoid the fluidity of the mortar or the cement paste being too high, resulting in segregation during testing, the polycarboxylate-based superplasticizer is not used in cement paste, and its dosage in mortar is less than that used in concrete, as shown in Table 1.

Test Apparatus and Procedure

A shear box test apparatus was developed to measure the shear flow of fresh concrete by applying arbitrary stress from zero. It was constructed as shown in Fig. 8, by linking five stainless steel frames with bearings to reduce the friction between the specimen and the shear box inside when the specimen deforms. The frictional resistance of this apparatus itself is shown in Fig. 9 under different vertical pressures that are applied to the top surface of the specimen. When the top frame of the shear box is horizontally pulled by a servomotor or a weight, two rotating plates revolve in the same direction, and a shear deformation is thus caused in the specimen (size: $L18\times W10\times H10$ cm). The vertical pressure applied to the top surface of specimen is adjusted by changing the plate-shaped weight.

Because the shear plane is characterized only by its direction, there are countless shear planes in the same direction. If regarding fresh concrete as uncompressible material (i.e., Poisson's ratio is 0.5), and ignoring the sliding resistance between the specimen and the shear box inside, the compressive stress acting on each side of the specimen is equal to that on its top surface. In this case, the specimen is in a sample shear state, and all the shear planes are horizontal, acted on by the same shear stress. The shear stress and the normal stress, acting on any shear plane are, respectively, as follows:

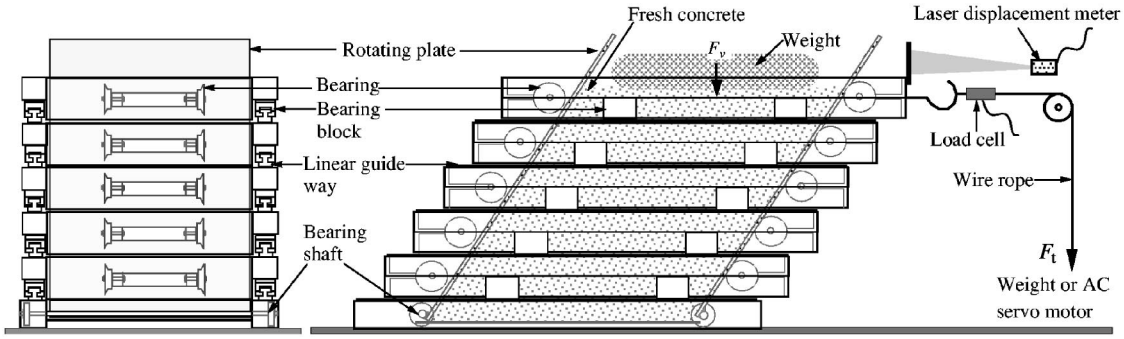

Fig. 8. Shear box test apparatus for cementitious materials in fresh state

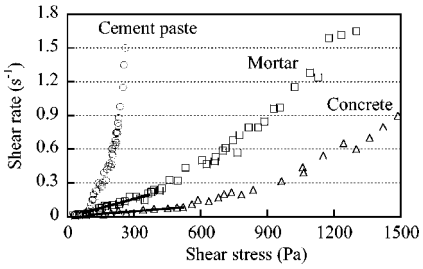

Fig. 10. Flow curves of high fluidity cementitious materials (T =285 K, F_v=0)

$$\tau = \frac{F_t}{0.1 \times 0.18} = 55.6F_t$$

$$\sigma_n = \frac{F_v}{0.1 \times 0.18} + \rho_c g h_x = 55.6F_v + \rho_c g h_x \tag{23}$$

where F_t = pulling force (N); F_v = vertical pressure of applied weight (N); ρ_c = unit mass of specimen (kg/m^3); g = gravity acceleration (=9.8 m/s^{-2}); and h_x = height from examined horizontal shear plane to specimen's top surface (m).

Eq. (23) indicates that the magnitude of normal stress varies with the position of horizontal shear plane. Thus, the shear rate changes along the height direction of the specimen even for a given shear stress. Hence, measured shear rate should be regarded as a mean value of the shear rates on all the horizontal shear planes, and it is equivalent to the shear rate under the mean normal stress (σ_{nm}) shown in the following equation:

$$\sigma_{nm} = 55.6F_v + \tfrac{1}{2}\rho_c g H \tag{24}$$

where H = specimen height (m).

As a test procedure, right after the specimen is mixed, it is packed into a polyethylene bag that was previously treated with lubricant, and placed into the shear box. Then a plate of a specified weight is placed on its top surface, and the horizontal pulling force is increased step by step from zero. Meanwhile, the pulling force and the horizontal displacement of the box's top frame are measured with a load cell and a laser displacement meter (LDM), respectively. When the top frame reaches a certain position, the test is over. Based on the measured results of time–load–shear displacement relationship, the shear stresses and the shear rates resulted at 10 ms after each stress is applied are, respectively, calculated and a shear rate–shear stress relational curve, i.e., a flow curve, is plotted. Forthermore, the apparent viscosity of the tested specimen under a selected shear rate is calculated. Since

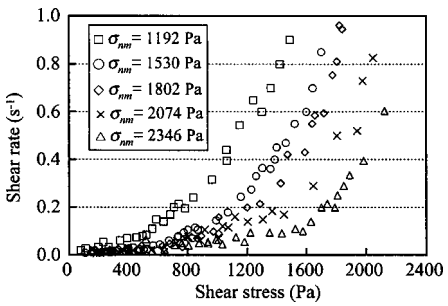

Fig. 11. Flow curve of high fluidity concrete under different mean normal stress levels (T=285 K)

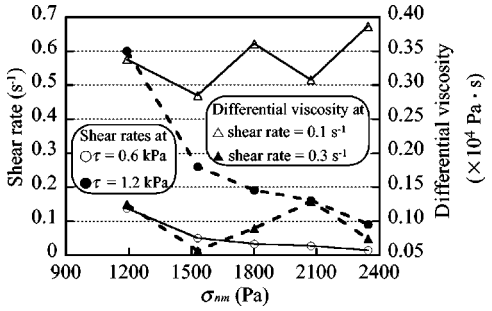

Fig. 12. Effects of mean normal stress on shear rate and differential viscosity of high fluidity concrete

horizontal pulling force of any magnitude can be applied by weights and the displacement is measured by the LDM, this apparatus of stress control type has the ability to precisely measure the flow curve of fresh concrete in a wide range of shear rate.

Test Results and Discussion

Fig. 10 shows flow curves measured for three kinds of high fluidity cementitious materials at a temperature of 12°C. The measured shear rates are up to 10 s^{-1}, but because the trend of the flow curve does not change above a certain shear rate, the plotted flow curves are only limited to the shear rate range of 0–1.8 s^{-1} to clearly show the character of the flow curve in the low shear rate region. As can be seen in this figure, none of the flow curves was a straight line, but the portion in the low shear rate region approximates a straight line, verifying Eqs. (12) and (15). The near-linear portion on the flow curve of the cement paste was so short that it can be ignored, and approximating the whole flow

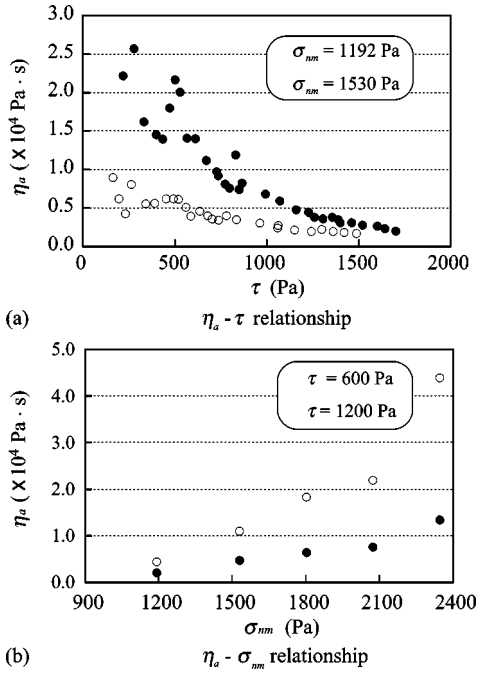

Fig. 13. Variations of apparent viscosity η_a with applied stress τ or σ_{nm} (T=285 K)

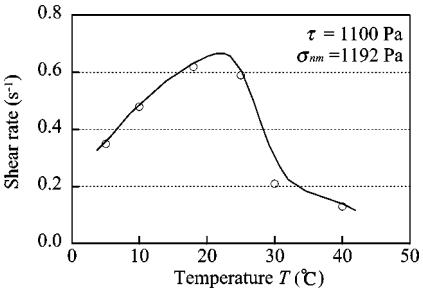

Fig. 14. Relationship between shear rate of high fluidity concrete and temperature

curve to a straight line does not cause much error. That is, the flow behavior of the cement paste approximately follows the Bingham model.

However, when aggregates were mixed into the cement paste, the portion in the low shear rate range of flow curve becomes longer so that the whole flow curve of high fluidity mortar or concrete has a large curvature. Hence, the characterization or prediction of the flow behavior with the linear model–Bingham model for high fluidity concrete will result in a great error.

Fig. 11 shows the measured flow curves in shear rate region of $0-1.0\ s^{-1}$ for the high fluidity concrete specimen under different vertical pressures. The flow curve shifted toward the right with increasing mean normal stress (σ_{nm}). Furthermore, as shown in Fig. 12, the shear rate decreased with increasing σ_{nm} for any given shear stress, but the differential viscosity at any given shear rate level was nearly unchanged. These experimental results were consistent with those obtained by the theoretical analyses.

Fig. 13 indicates that the apparent viscosity of high fluidity concrete increased with decreasing shear stress when fixing σ_{nm}, or with increasing σ_{nm} for a certain shear stress. Hence, the apparent viscosity of high fluidity concrete, being stress dependent, is a kind of structural viscosity in contrast to the stress-independent viscosity of Newtonian fluid.

Fig. 14 shows the measured shear rates of high fluidity concrete under different environmental temperature (T) when only a given horizontal pulling force was applied. For a given stress state, the shear rate increased with increasing T up to a certain limit, but when the T rose above this limit, the shear rate decreased with T. This is because the decrease in the viscosity of water and the increase in thermal motion energy of particles with T within the limit result in a greater reduction in the flow resistance of fresh concrete than the increase caused by the increased hydration. However, when T is higher than the limit, a larger amount of hydrate is created, and accordingly much free mixing water is exhausted, so that a greater increase in the flow resistance results. The shape of the $\dot{\gamma}-T$ relational curve shown in Fig. 14 agrees with that derived theoretically, as shown in Fig. 7(b).

Conclusions

In this study, the shear flow behavior of high fluidity concrete after yielding was quantitatively analyzed using a microscopic approach. The main conclusions are as follows:

1. High fluidity concrete can be thought as a kind of particle assembly composed of cohesive particles and cohesionless particles, and the relationship between particle movement and deformation of the particle assembly is as shown in Eq. (3).
2. The potential energy of cement particles results in the time dependence of the flow behavior of fresh concrete. The flow mechanism of fresh concrete can be clarified by applying expanded Eyring's viscosity theory.
3. The existence of interfriction causes the flow behavior of fresh concrete to depend on normal stress on the shear plane. With increasing normal stress, the shear rate decreases for a certain shear stress, and thus apparent viscosity increases. However, the differential viscosity does not change.
4. The flow curve of high fluidity concrete is not a straight line, and it is affected by environmental temperature, and normal stress, etc. besides concrete's composition. Apparent viscosity is dependent on the stress state. The Bingham model may approximately describe the flow behavior in the low shear rate range.
5. With increasing environmental temperature up to a certain limit, the flow performance of high fluidity concrete is improved. Once the temperature exceeds this limit, the fluidity drops.

Notation

The following symbols are used in this paper:

E_c = mean potential energy of cement particles;
N = number of particles in unit dimension of particle layer;
S_d = stress distribution coefficient;
η_a = apparent viscosity of fresh concrete;
θ_m = mean contact point angle of particle assembly;
Λ_m = mean moving distance of moving particles;
σ_n = normal stress on the shear plane;
τ = shear stress;
τ_y = yield stress; and
ϕ_m = mean inter-frictional angle of particle assembly.

References

Banfill, P. F. G. (1990). "Use of the viscocorder to study the rheology of fresh mortar." *Mag. Concrete Res.*, 42(153), 213–221.

Banfill, P. F. G. (1991). "The rheology of fresh mortar." *Mag. Concrete Res.*, 43(154), 13–21.

Everett, D. H. (2000). *Basic principles of colloid science*, The Royal Society of Chemistry, Kyoto, Japan, 23–27.

Fukaya, T. (1992). "The flowing behavior of fresh cement and concrete." *Cement Concrete, Japan Cement Association*, 540, 30–39.

Goto, K. (1963). *Rheology and application*, Kyoritsu Publishing House, Tokyo, 49–51.

Hu, C., and Larrard, F. D. (1996). "The rheology of fresh high-performance concrete." *Cem. Concr. Res.*, 26(2), 283–294.

Japan Rheology Society (1992). *Course of rheology*, Polymer Science Publishing Co. Ltd, Tokyo, 151–157.

Li, Z. G. (2001). "A study on the dependence of yield stress of high fluidity concrete on loading conditions." *Proc., 3rd Int. Conf. on Concrete under Severe Condition of Environment and Loading*, Vancouver, Canada, 1376–1383.

Li, Z. G., Tanigawa, Y., and Mori, H. (2002). "Theoretical analysis on time-dependence of fluidity and thixotropy of high fluidity concrete." *J. Struct. Constr. Eng.*, 542, 47–53 (in Japanese).

Li, Z. G., Tanigawa, Y., Mori, H., and Kurokawa, Y. (1999). "Study on constitutive law of fresh mortar using particle assembly model." *J. Struct. Constr. Eng.*, Architecture Institute of Japan, 523, 17–24.

Li, Z. G., Tanigawa, Y., Mori, H., and Ohkubo, T. (2001). "Study on limit stress at shear failure of fresh mortar by microscopic approach." *J.*

Struct. Constr. Eng., 542, 47–53.
Mori, H. (1998). "High fluidity concrete." *J. Architecture Building Sci.*, Architecture Institute of Japan, 113, (1420), 41–43.
Mori, H., Tanaka, M., and Tanigawa, Y. (1991). "Experimental study on the shear deformational behavior of fresh concrete." *J. Struct. Constr. Eng.*, 421, 1–10.
Murayama, T. (1991). *Theory of mechanical behavior of soil*, Gihodoshuppan Co. Ltd., Kyoto, Japan, 27–79.
Nakae, K. (2001). *Rheology science and application technology*, Fujitech System Co. Ltd., Tokyo, 108–181.
Onogi, S. (2000). *Rheology used for specialist in chemical field*, The Royal Society of Chemistry, Kyoto, Japan, 13–19.
Papo, A. (1988). "The thixotropic behavior of white portland cement pastes." *Cem. Concr. Res.*, 18(4), 595–603.
Sakai, E., and Dimon, M. (1996). "The dispersion mechanisms of AE high range water reducing agent." *Cement Concrete*, 595, 13–22.
Shimada, K., Fujii, H., and Nishimura, S. (1993). "Increase of shear strength due to surface tension and suction of pore water in granular material." *Proc., Symp. on Mechanical Behaviors of Granular Material*, Japan, 17–20.
Struble, L. J., and Schultz, M. A. (1993). "Using creep and recovery to study flow behavior of fresh cement paste." *Cem. Concr. Res.*, 23(6), 1369–1379.
Tanigawa, Y., and Mori, H. (1988). "Toward the development of workability design of fresh concrete." *Cement Concrete*, 501, 11–20.
Tattersall, G. H., and Banfill, P. F. G. (1983). "The rheology of fresh concrete." Pitman Advanced Publishing Program, 330–360.
Uchikawa, H., Hanehara, S., and Sawaki, O. (1997). "Effect of electrostatic and steric repulsive force of organic admixture on the dispersion of cement particles in fresh cement paste." *Cement Concrete*, 602, 28–38.
Wallevik, O. H., and Gjørv, O. E. (1990). "Modification of the two-point workability apparatus." *Mag. Concrete Res.*, 42(152), 135–142.
Yamamoto, Y., Homma, A., and Kitsutaka, Y. (1996). "Study on the testing method of the rheological characteristic of high fluidity concrete." *J. Struct. Construction Eng.*, Architecture Institute of Japan, 489, 9–16.